Journal of Photochemistry and Photobiology 26-27 (2025) 100260

Contents lists available at ScienceDirect

Journal of Photochemistry and Photobiology

journal homepage: www.sciencedirect.com/journal/journal-of-photochemistry-and-photobiology

Effect of Er:YAG laser bone bed milling, with or without photobiomodulation, on the bone repair process of additive manufacturing implants in rats

Fernando Costa Neto [a], Isadora Breseghello [b,*], Laura Vidoto Paludetto [b], Sabrina Cruz Tfaile Frasnelli [b], Fábio Roberto de Souza Batista [b], Alberto Blay [c], Armando Boni [d], Fernando Costa Júnior [a], Roberta Okamoto [b,*]

[a] Program in Laser Dentistry, Catholic University of the Sacred Heart, Largo Francesco Vito, 1, 00168, Rome, Italy
[b] Department of Basic Sciences, Araçatuba Dental School, São Paulo State University Júlio de Mesquita Filho – UNESP, 16015-050, Araçatuba, SP, Brazil
[c] Plenum Bioengineering, Ain Ata Avenue, 640 - Jardim Ermida I, 13212-213, Jundiaí, SP, Brazil
[d] Beauty Smile – Laser dental health with Fotona, Des. Eliseu Guilherme street, 53/69 - Paraíso, 04004-030, São Paulo, SP, Brazil

ARTICLE INFO

Keywords:
Osseointegration
Laser Therapy
Dental Implantation
Osteocalcin
Photobiomodulation

ABSTRACT

The preparation of the bone bed for implant placement is a critical factor for successful osseointegration and is influenced by surgical techniques and instrumentation. In this context, a study was conducted to compare bone bed milling using an Er:YAG laser, with or without photobiomodulation, to conventional milling combined with Nd:YAG laser photobiomodulation. To assess the effects of Er:YAG laser milling, with or without photobiomodulation, on bone bed preparation and its potential to enhance osseointegration, 28 male rats underwent implant placement in their tibial metaphyses and were divided into four groups: conventional milling (CM), photobiomodulation + conventional milling (PBM + CM), Er:YAG laser milling (Er:YAG), and photobiomodulation + Er:YAG laser milling (PBM + Er:YAG). Euthanasia was performed 28 days after implant placement. Reverse torque testing and real-time PCR (RT-PCR) analysis were conducted to evaluate the expression of osteogenic markers, including ALP, IBSP, OCN, and RUNX2. Data were analyzed using the Shapiro-Wilk test, followed by one-way ANOVA and Tukey's post hoc test, where applicable, with a significance level of $p \leq 0.05$. The Er:YAG group exhibited a significantly higher implant removal torque compared to the CM group. Additionally, the expression of genes associated with bone maturation (OCN), differentiation (RUNX2), and osteoblastic activity (ALP and IBSP) was significantly increased in both the Er:YAG and PBM + Er:YAG groups, indicating enhanced osteogenic potential. Thus, Er:YAG laser milling, with or without photobiomodulation using the Nd:YAG laser, may represent a promising alternative for bone bed preparation in implant procedures. However, further studies are required to better characterize bone healing and its long-term consolidation.

1. Introduction

Significant advancements in implant dentistry have transformed the ability to restore dental function and aesthetics, making dental implants a common and highly effective procedure in clinical practice. Achieving successful outcomes in implant therapy requires a thorough understanding of the osseointegration process and the factors that influence it. Among these factors, the preparation of the bone bed plays a pivotall role, as it establishes the foundation for the integration of the implant with the surrounding bone tissue [1,2].

Conventional bone bed preparation primarily relies on rotary instruments, a well-established technique that follows standardized protocols to ensure efficacy and safety. However, this method presents several challenges, including drill wear and the formation of an amorphous layer of bone debris on the bone surface after drilling. This debris may act as a physical barrier, impeding the interaction between blood components and the underlying bone tissue, potentially delaying osseointegration [3]. Furthermore, precise control of parameters such as revolutions per minute (RPM) and local cooling is essential to prevent overheating, which can result in protein denaturation, enzyme

* Corresponding authors.
E-mail addresses: isadora.breseghello@unesp.br (I. Breseghello), roberta.okamoto@unesp.br (R. Okamoto).

https://doi.org/10.1016/j.jpap.2025.100260

Available online 25 March 2025

inactivation, and bone necrosis [4].

Given these limitations, research into alternative bone bed preparation methods is crucial for enhancing the predictability, safety, and efficacy of implant procedures. One promising approach involves the use of laser technology, which offers distinct advantages over conventional rotary instruments. Notably, the Er:YAG (Erbium-Yttrium Aluminum Garnet) and Nd:YAG (Neodymium-Yttrium Aluminum Garnet) lasers have demonstrated potential in optimizing bone bed preparation. These technologies provide high precision with minimal invasiveness, potentially improving biological responses while reducing thermal and mechanical trauma [5]. Several preclinical animal studies investigating laser-assisted bone bed milling have reported favorable outcomes [6,7].

The Er:YAG laser, operating at a wavelength of 2,940 nm, aligns with the absorption peaks of water and hydroxyapatite, enabling precise and clean bone ablation with minimal thermal damage [8,9]. This laser significantly reduces bone debris formation and eliminates the need for direct contact with the tissue, thereby minimizing contamination risks and creating a more favorable environment for osseointegration. By preserving adjacent bone structures and exposing a debris-free mineralized matrix, the Er:YAG laser may promote enhanced healing and osseointegration [10]. The osteotomy effects of the Er:YAG laser have been recognized for decades [11,12].

Similarly, the Nd:YAG laser, which operates at 1,064 nm, exhibits high tissue penetration and significant potential for photobiomodulation. While its primary applications include soft tissue management and peri-implant decontamination, studies suggest that it may also influence bone regeneration and remodeling [13,14]. Its photothermal and hemostatic properties contribute to improved surgical outcomes by promoting controlled healing and minimizing bleeding [15].

Continued preclinical investigations into the application of lasers in bone bed preparation will be crucial for defining optimal parameters and evaluating their effects on tissue response, bone remodeling, and overall osseointegration quality, ultimately paving the way for more advanced and less invasive implant techniques [16]. Laser-assisted bone drilling for dental implant placement emerges as a promising technique for preparing the bone bed, allowing for precise and minimally invasive cuts while reducing thermal and mechanical trauma to the surrounding tissues [17]. The present study aimed to analyze bone repair following bone bed drilling and dental implant placement in the tibiae of male rats using an Er:YAG laser, with or without the Nd:YAG laser.

2. Methods

2.1. Animals

With the approval of the Research Ethics Committee on the Use of Animals of the Faculty of Dentistry of Araçatuba-UNESP (FOA process n° 710-2023), 28 male rats (Rattus norgicus albinus, Wistar), aged 3 months, were used in this study. All animal experiments were in accordance with ARRIVE (Animal Research: Reporting of In Vivo Experiments) guidelines and with the NIH (National Research Council) Guide for the Care and Use of Laboratory Animals. The rats were equally and randomly divided into experimental groups according to the type of bone bed milling and its association with oy without photobiomodulation with Nd:YAG. All the experimental groups contained 7 animals, as follows: CM (conventional milling): group in which the bone bed was milled with a conventional metal cutter - $n = 7$; PBM + CM (photobiomodulation + conventional milling): group in which the bone bed was milled with a conventional metal cutter combination with photobiomodulation with Nd:YAG - $n = 7$; Er:YAG (milling with Er:YAG): group in which the bone bed was milled with Er:YAG - $n = 7$ and PBM + Er:YAG (photobiomodulation + Er:YAG): group in which the bone bed was milled with Er:YAG combination with photobiomodulation with Nd:YAG - $n = 7$. All experimental groups were euthanized at 28 days after surgery.

2.2. Experimental model design

On day 0, the rats selected for the experiment underwent implant installation surgery in the tibial metaphyses. At 28 days post-implant placement (day 28), the animals were euthanized for reverse torque (RT) testing and real-time PCR (RT-PCR) analysis.For this purpose, the animals were identified using a numerical sequence and randomly assigned to one of two groups (Micro-CT and RT-PCR), with randomization performed using Excel 2016 software (Fig. 1).

2.2.1. Implants used in this research

Commercially pure-grade IV titanium implants based on the concept of double-acid etching (Plenum ®, Jundiaí, SP, Brazil) with a diameter of 1.4 mm and height of 2.7 mm were used. The implants were sterilized by gamma irradiation. Plenum ® dental implants use innovative technologies by incorporating additive manufacturing or 3D printing into the manufacturing process. The entire implant design is carried out on digital platforms. The additive manufacturing process gives the part special characteristics, such as roughness and resolution of implant details. These surface characteristics make it possible to mimic the microstructure of bone tissue (trabeculae), controlled wettability, allowing the concentration of growth factors and easy cell adhesion [18].

2.2.2. Surgery to place osseointegrable implants in the Tibia

The animals were fasted for 8 hours prior to surgery and anesthetized intramuscularly with 50 mg/kg of ketamine hydrochloride (ketamine hydrochloride injectable, Vetnil, Louveira, SP, Brazil) and 5 mg/kg of xylazine hydrochloride (2 % xylazine hydrochloride injectable, Syntec, Tamboré, SP, Brazil). After anesthesia, a trichotomy was performed on the medial part of both the right and left tibiae. The incision area was aseptically prepared with Povidone-Iodine Germicidal Solution (10 % Povidone-Iodine, Riodeine Germicidal, Rioquímica, São José do Rio Preto, SP, Brazil) combined with topical Povidone-Iodine.

Using a no. 15 blade (Feather Industries Ltd., Tokyo-To, Japan), an approximately 1 cm incision was made in the region of the left and right tibial metaphyses, and then the soft tissues were dissected and retracted with periosteal elevators, exposing the bone to receive the implants. A total of 56 commercial-grade IV titanium implants, 1.4 mm in diameter and 2.7 mm in height, sterilized by gamma irradiation, were placed (2 per animal). In the CM group, milling was performed in both cortices with a 1.1 mm diameter spiral drill attached to an electric motor (BLM600®; Driller, São Paulo, SP, Brazil) at a speed of 1000 rpm, under irrigation with isotonic sodium chloride solution 0.9 % (Physiological®, Laboratórios Biosintética Ltd., Ribeirão Preto, SP, Brazil), and a 20:1 reduction contra-angle handpiece (Angular piece 3624N 1:4, Head 67RIC 1:4, KaVo®, Kaltenbach & Voigt GmbH & Co., Biberach, Germany). In the PBM + CM group, milling was carried out in the same way as in the CM group, but photobiomodulation was performed with an Nd:YAG laser (LightWalker AT, Fotona®, Slovenia), with a wavelength of 1064 nm, immediately beforehand. The treatment was applied using the MarCo™S handpiece, with a power density of 0.127 W/cm^2, total energy of 6J, 10mm spot size, a frequency of 10 Hz and MSP pulse mode (100 μs) and energy output per pulse of 10mJ over the beam spot size for 60 seconds before conventional milling. Only one point of irradiation was performed, in the region of the tibial metaphysis, where milling was subsequently carried out to install the implants. In the Er:YAG group, the bone bed was milled using the Er:YAG laser (LightWalker AT, Fotona®, Slovenia) with a wavelength of 2940 nm. The procedure used the H-14 handpiece equipped with a TIP Conical Sapphire 800/12, delivering 200 mJ of energy and energy density per pulse of 2.5J/cm^2/pulse at a frequency of 15 Hz, with an average power of 3 W. The laser operated in QSP pulse mode, with water set at power level 0, since irrigation was performed manually with 0.9 % sodium chloride, to mimic the

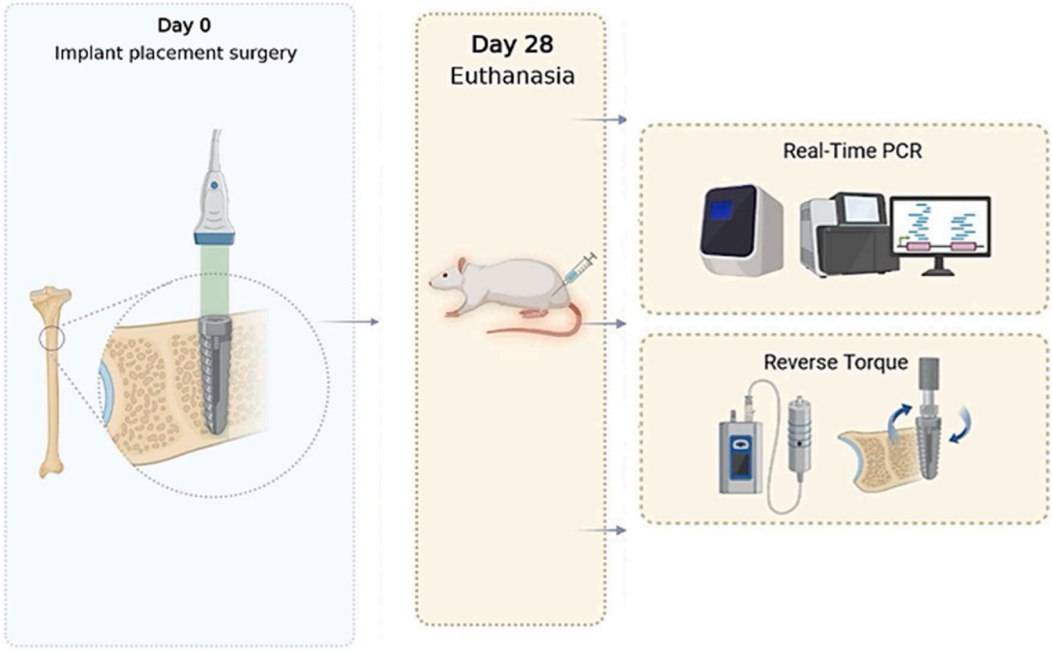

Fig. 1. Schematic drawing illustrating the experimental design of the study.

conditions of irrigation carried out in manual milling, air at power level 5, under irrigation with 0.9 % isotonic sodium chloride solution (Fisiológico®, Laboratórios Biosintética Ltda.a®, Ribeirão Preto, SP, Brazil). Approximately 15 seconds were required for each bone milling, with a variation of approximately 5 seconds more or less, depending on the thickness of the tibia.

In the PBM + Er:YAG group, milling was also performed in the same way as in the Er:YAG group; however, photobiomodulation was performed just before, with the same parameters used in the PBM + CM group. In all experimental groups, tissues were sutured in layers with interrupted sutures, using monofilament sutures (Nylon 5.0, Ethicon, Johnson & Johnson, São José dos Campos, SP, Brazil) for the inner layers and multifilament sutures (Silk 4-0, Ethicon, Johnson & Johnson, São José dos Campos, SP, Brazil) for the outermost layer. Immediately postoperatively, each animal received an intramuscular dose of 0.2 mL of Benzathine Penicillin G (Pentabiótico Veterinary Small Size, Fort Dodge Animal Health Ltd., Campinas, SP, Brazil).

2.2.3. Euthanasia

The animals were euthanized by anesthetic overdose 28 days after implant placement (day 28). Bilateral tibiae were harvested for reverse torque (RT) and RT-PCR analysis.

2.2.4. Biomechanical analysis – removal torque (RT)

For removal torque analysis, the implants exposed in the specimens were connected to a digital torque tool. A counterclockwise movement was applied, gradually increasing the removal torque until the implant rotated within the bone tissue and the bone-implant contact was completely broken. The device recorded the maximum peak torque for this fracture in newton-centimeters (N/cm), and the values were pooled and subjected to statistical analysis.

2.2.5. Molecular analysis – real-time PCR (RT-PCR)

Immediately after the removal of the implants from the tibia and using reverse torque, peri-implant bone was collected with mini gouge forceps. A safety margin of 0.5 cm of bone was maintained around the peri-implant region during the collection to ensure that the bone remained safely in contact with the implant coils, which is the bone of interest for RT-PCR analysis.

The bone was carefully washed in phosphate-buffered saline, frozen in liquid nitrogen, and stored at −80°C for total RNA extraction using Trizol reagent (Life Technologies: Invitrogen, Carlsbad, CA, USA). After analyzing RNA integrity, purity, and concentration, cDNA was synthesized using 1 μg of RNA via a reverse transcriptase reaction (M-MLV reverse transcriptase: Promega Corporation, Madison, WI, USA). Sample cDNA was pipetted onto the array PCR plate with TaqMan Fast Advanced Mastermix (Applied Biosystems, Foster City, CA, USA) to detect genes involved in the bone repair process (TaqMan Array Fast 96 well plate, Applied Biosystems). Real-time PCR was performed on a Step One Plus real-time PCR detection system (Applied Biosystems) under the following conditions: 50°C (2 min), 95°C (10 min), 40 cycles of 95°C (15 s), and 60°C (1 min), followed by a standard denaturation curve. Relative gene expression was calculated by referencing mitochondrial ribosomal protein expression and normalized by the gene expression of tibia fragments undergoing repair during different experimental periods (ΔΔCT method). The assay was performed in quadruplicate, and the genes evaluated were Runt-related transcription factor 2 (RUNX2), osteocalcin (OCN), alkaline phosphatase (ALP), and bone sialoprotein (IBSP), with beta-actin (BACT) as a constitutive control. The values obtained from the proposed analyses were submitted to statistical analysis using GraphPad Prism 7.03 software. The test for homoscedasticity was the Shapiro–Wilk test, and the normal distribution of the data was confirmed for all parameters analyzed. Next, the one-way ANOVA test was performed. Subsequently, Tukey's post-test was conducted with a significance level of $p \leq 0.05$ to identify the differences between the groups.

2.2.6. Statistical analysis

The data obtained from the analysis of reverse-torque (RT) and RT-PCR were subjected to statistical analysis using GraphPad Prism 7.03 software. After applying the Shapiro-Wilk test for normality and confirming the normal distribution of the data, they were subjected to the parametric one-way analysis of variance (one-way ANOVA), followed by Tukey's post-test, when necessary, to determine the differences observed between the evaluated groups. The significance level was set at 5 % ($p \leq 0.05$).

The dependent variable used to determine the sample size was BV/TV, and the data were taken from the article by Gomes-Ferreira et al.

[19]. The sample size for this study for each group was determined using the power test via the website http://www.openepi.com/SampleSize/SSMean.htm. Based on previously published results, the means used for the calculation were 33.37 and 43.54, with standard deviations of 8.53 and 5.77, at a significance level of 5 % and a power of 95 % in a one-tailed hypothesis test. As such, a sample size of 7 animals per group was required. The estimate for each outcome measure was made to achieve a power of 0.8 and an alpha error of 0.05.

3. Results

3.1. Biomechanical analysis - removal torque (RT)

There was a statistically significant difference in removal torque values between the CM and Er:YAG groups (p = 0.0218). On the other hand, no statistically significant differences were observed between the CM, PBM + CM, CM, PBM + Er:YAG, PBM + CM, and PBM + Er:YAG groups, as shown in Fig. 2.

3.2. Molecular analysis - real-time PCR (RT-PCR)

There was a statistically significant difference in the gene expression of OCN between the following groups: CM vs. Er:YAG and CM vs. PBM + Er:YAG ($p \leq 0.05$). However, no statistically significant differences were observed between the CM vs. PBM + CM, PBM + CM vs. Er:YAG, and PBM + CM vs. PBM + Er:YAG groups. Mean values of the groups: CM (1.005 ± 0.120), PBM + CM (2.215 ± 0.640), Er:YAG (4.781 ± 0.673), and PBM + Er:YAG (3.644 ± 1.84) (Fig. 3a).

There was a statistically significant difference in the gene expression of RUNX2 between the following groups: PBM + CM vs. PBM + Er:YAG ($p \leq 0.005$). However, no statistically significant differences were observed between the CM vs. PBM + CM, CM vs. Er:YAG, CM vs. PBM + Er:YAG, PBM + CM vs. Er:YAG, and Er:YAG vs. PBM + Er:YAG groups. Mean values of the groups: CM (1.117 ± 0.204), PBM + CM (0.6497 ± 0.162), Er:YAG (1.139 ± 0.208), and PBM + Er:YAG (1.596 ± 0.49) (Fig. 3b).

There was a statistically significant difference in the gene expression of ALP between the CM vs. Er:YAG, CM vs. PBM + Er:YAG, and PBM + CM vs. PBM + Er:YAG groups ($p \leq 0.005$). However, no statistically significant differences were observed between the CM vs. PBM + CM, PBM + CM vs. Er:YAG, and Er:YAG vs. PBM + Er:YAG groups. Mean values of the groups: CM (1.003 ± 0.081), PBM + CM (1.117 ± 0.108), Er:YAG (1.272 ± 0.211), and PBM + Er:YAG (1.689 ± 0.489) (Fig. 3c).

There was a statistically significant difference in the gene expression of IBSP between the CM vs. PBM + Er:YAG and between the PBM + CM vs. PBM + Er:YAG groups ($p \leq 0.005$). However, no statistically significant differences were observed between the CM vs. PBM + CM, CM vs. Er:YAG, PBM + CM vs. Er:YAG, and Er:YAG vs. PBM + Er:YAG groups. Mean values of the groups: CM (1.002 ± 0.072), PBM + CM (1.134 ± 0.211), Er:YAG (1.526 ± 0.138), and PBM + Er:YAG (1.620 ± 0.372) (Fig. 3d).

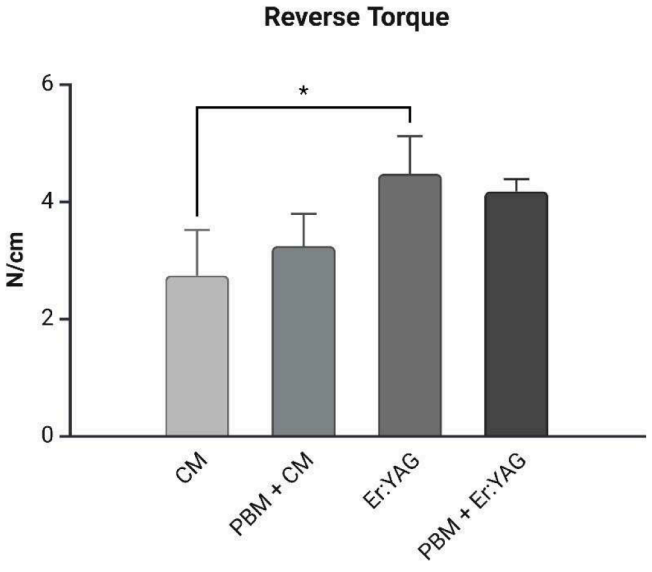

Fig. 2. Mean removal torque values between the CM, PBM + CM, ER:YAG and PBM + ER:YAG groups. Mean values: CM (2.733 N/cm ± 0.7767), PBM + CM (3.233 N/cm ± 0.5508), ER:YAG (4.467 N/cm ± 0.6429) and PBM + ER:YAG (4.167 N/cm ± 0.2083). *: statistically significant difference ($p \leq 0.05$).

4. Discussion

The concept of laser surgery represents a significant advancement in addressing key clinical challenges in bone milling. The elimination of frictional heat, a common issue in conventional methods, preserves bone tissue from thermal damage, thereby promoting better conditions for bone repair and integration [20,21]. Additionally, the absence of vibrations during surgery contributes to a more stable milling process [22].

The present in vivo study in experimental animals compared different milling techniques in the tibias of male rats, classified into the CM, PBM+CM, Er:YAG, and PBM+Er:YAG groups, as previously described. To assess the effects of high-intensity laser on bone formation following milling and implant placement, we evaluated its impact on trabecular bone using biomechanical analysis (reverse removal torque) and real-time PCR analysis.

The results of the biomechanical analysis of removal torque (RT) indicated a statistically significant difference between the CM (conventional milling) and Er:YAG (Er:YAG laser) groups, with the Er:YAG group showing significantly higher removal torque values (p = 0.0218). We hypothesize that, initially, conventional milling likely provided greater primary stability in the CM group due to the presence of a compacted bone layer at the periphery of the bone bed—a condition that does not occur in the laser bone ablation process [23]. However, throughout the peri-implant bone repair process, the Er:YAG laser may have facilitated a more effective interaction between the bone itself and the implant. Since laser milling does not produce a compacted bone layer, this may have enhanced the migration of osteoprogenitor cells to the implant surface, promoting contact osteogenesis in the Er:YAG group. Consequently, this process could have improved secondary stability, leading to higher removal torque values at 28 days postoperatively.

On the other hand, no statistically significant differences were observed in the removal torque between the groups that combined photobiomodulation (PBM) with the conventional or laser milling techniques. Photobiomodulation, known for its cell-stimulating action, may have neutralized the differences between the milling techniques, providing a compensatory effect that favored bone regeneration in a similar way among the treated groups.

Real-time PCR (RT-PCR) data showed a significant difference in RUNX2 gene expression between the PBM + CM and PBM + Er:YAG groups, with an increase in RUNX2 gene expression in the PBM + Er:YAG group compared to the PBM + CM group. This suggests that the combination of Er:YAG laser and photobiomodulation (PBM) has a more pronounced impact on the activation of RUNX2[24], a key gene for osteoblast differentiation and bone formation. The increased expression of RUNX2 may indicate that this combination creates a more favorable environment for bone regeneration.

In the case of the OCN gene, expression was significantly higher in the Er:YAG and PBM + Er:YAG groups compared to the other groups. This result corroborates the findings of the biomechanical analysis of reverse torque, as higher OCN gene expression values indicate, among other factors, greater mineralization of bone tissue [25]. The results for the ALP and IBSP genes were similar, with better outcomes in the Er:

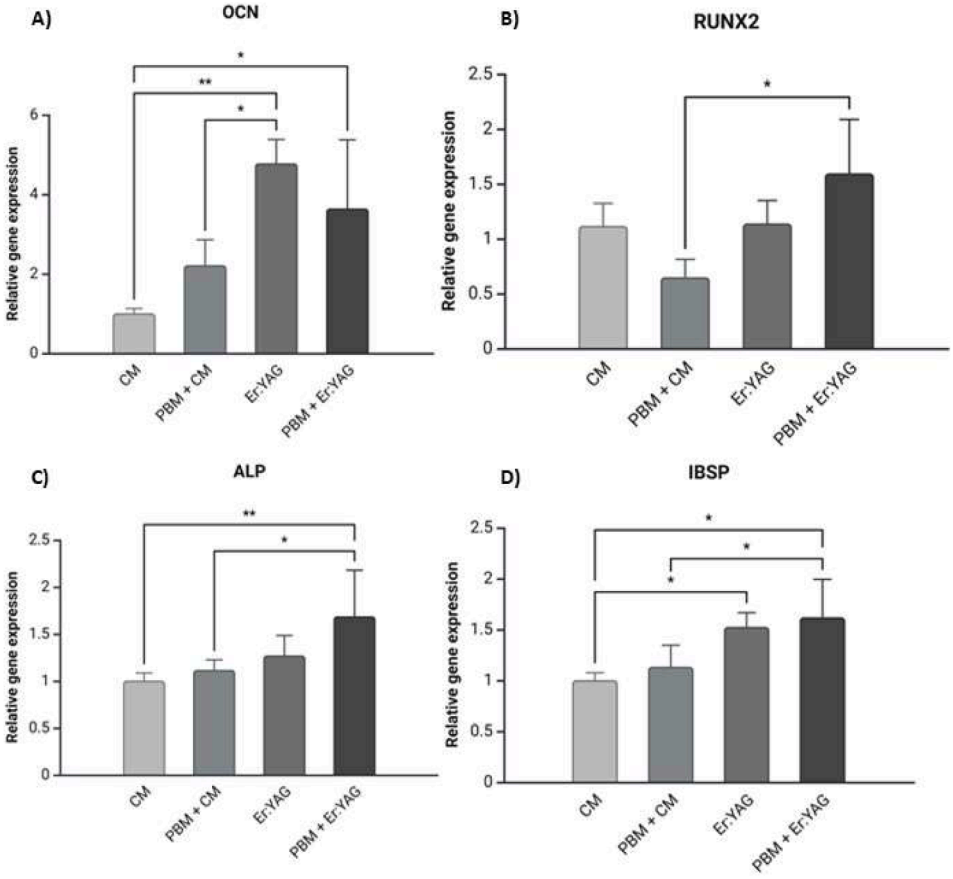

Fig. 3. Results of RT-PCR analysis (mean and standard deviation) for the CM, PBM + CM, Er:YAG and PBM + Er:YAG groups *: statistically significant difference ($p \leq 0.05$). **: statistically significant difference ($p \leq 0.005$).

YAG and Er:YAG + Nd:YAG groups. The OCN gene is a marker of osteoblastic maturation [26], while the IBSP and ALP genes are markers of osteoblastic activity [27,28]. Increased expression of these genes in the groups treated with Er:YAG and PBM suggests that laser application, particularly when combined with PBM, can accelerate osteogenesis and improve bone quality around the implant. These findings support the idea that combining laser techniques with photobiomodulation can enhance bone formation and improve implant integration [29].

In an animal study evaluating the impact of Nd:YAG laser application on the repair of rat tibial defects, favorable results were observed compared to the control group. According to the authors, the laser stimulated bone formation during the initial repair period [30].

The biomechanical and molecular results suggest that the use of the Er:YAG laser may be a promising alternative to the traditional manual rotary system (conventional milling), especially in contexts where the initial stability of the implant is a concern [31]. Milling with the Er:YAG laser indicated greater implant removal torque, and its use demonstrated a more favorable biological response, with increased induction of osteogenic genes such as RUNX2 and OCN.

As gene expression in real-time PCR indicates potential future responses, we hypothesize that these more favorable biological responses could translate into bone neoformation and mineralization. This suggests that, in a later euthanasia period, an increase in reverse torque values could also be observed in the PBM + Er:YAG group.

Thus, Er:YAG may represent a future alternative to the manual rotary method, potentially offering the advantage of inducing a biological response favorable to bone regeneration and implant integration. The hypothesis is that this approach could improve the mechanical stability of the implant with less thermal damage to the bone tissue and greater control during the preparation of the bone bed. Photobiomodulation with the Nd:YAG laser could complement the process, promoting better healing and osseointegration conditions. However, further studies are needed to understand the optimal settings and interactions between these techniques in order to maximize their clinical benefits.

Finally, despite the potential benefits of using the Er:YAG laser to prepare the bone bed for implants, its clinical application still faces some limitations. One of the main challenges is the higher cost associated with laser technology, both in acquiring the equipment and in maintaining it, making its implementation less accessible for routine dental practice. Additionally, the dimensional accuracy of the bone bed created by the laser may be inferior to that obtained with manual cutters for certain implant designs, especially conical implants, as the laser beam is cylindrical. This could compromise the primary stability of the implant, particularly in immediate loading protocols. The technique would also require longer operative time and a steeper learning curve to ensure its effective and safe application. These factors should be considered when assessing the feasibility of using the Er:YAG laser in the clinical context.

5. Conclusion

Thus, the results of this preliminary in vivo study indicate that the use of the Er:YAG laser, with or without photobiomodulation (PBM) using the Nd:YAG laser, appears to be a promising future alternative for preparing the bone bed for the installation of osseointegrable implants. However, further analyses and studies are needed to investigate the cellular and structural responses of bone tissue to its use, long-term bone healing, and the longevity of implants installed using this technique.

6. Limitations of the study

As the initial objective of this study was to conduct a preliminary analysis of the biological and mechanical responses to laser milling, further histological analysis is required to better characterize the tissue response. Additionally, the study did not include later euthanasia periods, which would allow for the observation of long-term bone repair. This study also did not compare the increase in bone bed temperature during different types of milling, and it is not possible to conclude that the Er:YAG laser has provided favorable results in this regard. Finally, the study did not evaluate peri-implant bone repair in the different groups when applying load to the implants, which is a critical assessment for studying the longevity of the technique.

Funding information

This research was funded by Coordenação de Aperfeiçoamento de Pessoal de Nível Superior do Ministério da Educação (CAPES), grant number 2022/07158-8 and 2023/05814-8. Also, Roberta Okamoto is affiliated with the Research Productivity Scholarship (process: 308408/2023-3). Also, M3 Health Ind. Com. de Prod. Med. Odont. e Correlatos S. A., Jundiaí, Brazil for providing the implants and Beauty Smile - Laser Fotona® for supplying the Light Walker® device.

Ethical statement

The procedures were reviewed and approved by the institutional ethics committee on animal care (CEUA/FOA, protocol n° 710-2023).

Data availability statement

The authors will make the raw data supporting this article's conclusions available upon request.

CRediT authorship contribution statement

Fernando Costa Neto: Writing – review & editing, Visualization, Resources, Methodology, Investigation, Funding acquisition. **Isadora Breseghello:** Writing – review & editing, Writing – original draft, Visualization, Methodology, Formal analysis. **Laura Vidoto Paludetto:** Writing – review & editing, Writing – original draft, Visualization, Software, Methodology, Formal analysis. **Sabrina Cruz Tfaile Frasnelli:** Visualization, Methodology, Formal analysis. **Fábio Roberto de Souza Batista:** Visualization, Methodology, Formal analysis. **Alberto Blay:** Resources, Methodology, Funding acquisition. **Armando Boni:** Methodology. **Fernando Costa Júnior:** Resources, Investigation, Funding acquisition, Conceptualization. **Roberta Okamoto:** Visualization, Validation, Supervision, Resources, Project administration, Methodology, Funding acquisition, Formal analysis, Data curation, Conceptualization.

Declaration of competing interest

The authors declare that they have no known competing financial interests or personal relationships that could have appeared to influence the work reported in this paper.

Acknowledgements

The authors would like to thank the Fundação Coordenação de Aperfeiçoamento de Pessoal de Nível Superior (CAPES) for supporting this study (Funding Code 001). M3 Health Ind. Com. de Prod. Med. Odont. e Correlatos S.A., Jundiaí, Brazil for providing the implants. Beauty Smile - Laser Fotona® for supplying the Light Walker® device. Multiuser Laboratory of the Araçatuba-UNESP School of Dentistry and FINEP (FINEP/CT-INFRA-FINEP Agreement: 01.12.0530.00-PROINFRA 01/2011). In addition, this study was also supported by CNPq (process: 150297/2025-4) - National Council for Scientific and Technological Development - INCT Saúde Oral e Odontologia - Grants n° 406840/2022-9.

Data availability

Data will be made available on request.

References

[1] M. Sharawy, C.E. Misch, N. Weller, S. Tehemar, Heat generation during implant drilling: the significance of motor speed, J. Oral Maxillofac. Surg. 60 (10) (2002) 1160–1169, https://doi.org/10.1053/joms.2002.34527. Oct.
[2] J.B. Park, E.Y. Kim, J. Paek, Y.A. Kook, D.M. Jeong, I.S. Cho, et al., Primary stability of self-drilling and self-tapping mini-implant in tibia of diabetes-induced rabbits, Int. J. Dent. [Internet] 429359 (2014) 1–8, https://doi.org/10.1155/2014/429359 [cited 2025 Jan 9]Available from.
[3] G.E. Romanos, N. Gutknecht, S. Dieter, F. Schwarz, R. Crespi, A. Sculean, Laser wavelengths and oral implantology, Lasers Med. Sci. 24 (6) (2009) 961–970, https://doi.org/10.1007/s10103-009-0676-1. Nov.
[4] N. Kanazirski, D. Vladova, D. Neychev, R. Raycheva, P. Kanazirska, Effect of Er laser exposure on the amorphous wear layer in the marginal zone of the osteotomy site for screw-type dental implant placement: a histomorphological study, J. Funct. Biomater 14 (7) (2023) 376, https://doi.org/10.3390/jfb14070376. Jul 18.
[5] T. Ninomiya, Y. Miyamoto, T. Ito, A. Yamashita, M. Wakita, T. Nishisaka, High-intensity pulsed laser irradiation accelerates bone formation in metaphyseal trabecular bone in rat femur, J. Bone Miner. Metab. 21 (2) (2003) 67–73, https://doi.org/10.1007/s007740300011.
[6] T. Shimohira, S. Katagiri, Y. Ohsugi, T. Hirota, M. Hatasa, K. Mizutani, K. Watanabe, H. Niimi, T. Iwata, A. Aoki, Comprehensive and sequential gene expression analysis of bone healing process following Er:YAG laser ablation, Photobiomodul. Photomed. Laser. Surg. 39 (2) (2021) 100–112, https://doi.org/10.1089/photob.2020.4833. FebEpub 2020 Dec 21. PMID: 33347788.
[7] D.G. Panduric, I.B. Juric, S. Music, K. Molčanov, M. Sušic, I. Anic, Morphological and ultrastructural comparative analysis of bone tissue after Er:YAG laser and surgical drill osteotomy, Photomed. Laser Surg. 32 (7) (2014) 401–408, https://doi.org/10.1089/pho.2014.3711. JulPMID: 24992274.
[8] J. Zeitouni, B. Clough, S. Zeitouni, M. Saleem, K. Al Aisami, C. Gregory, The effects of the Er laser on trabecular bone micro-architecture: comparison with conventional dental drilling by micro-computed tomographic and histological techniques, F1000Res 6 (2017) 1133, https://doi.org/10.12688/f1000research.12018.1. Jul 17.
[9] J.T. Walsh Jr, T.J. Flotte, T.F. Deutsch, Er:YAG laser ablation of tissue: effect of pulse duration and tissue type on thermal damage, Lasers Surg. Med. 9 (4) (1989) 314–326, https://doi.org/10.1002/lsm.1900090403. PMID: 2761327.
[10] A. Hindy, F. Farahmand, FS. Tabatabaei, In vitro biological outcome of laser application for modification or processing of titanium dental implants, Lasers Med. Sci. 32 (5) (2017) 1197–1206. Apr 27.
[11] U.K. Akyol, M. Güngörmüs, C. Gündogdu, H. Erdem, Histologic evaluation of the effects of Er:YAG laser on bone ablation, J. Contemp. Dent. Pract. 10 (5) (2009) E065–E072. Sep 1PMID: 19838612.
[12] U. Akyol, M. Güngörmüş, Er:YAG laser ablation of bone in experimental diabetics, Photomed. Laser Surg. 28 (4) (2010) 477–482, https://doi.org/10.1089/pho.2008.2479. AugPMID: 19795995.
[13] I. Fragkioudakis, A. Kallis, E. Kesidou, O. Damianidou, D. Sakellari, I. Vouros, Surgical treatment of peri-implantitis using a combined Nd: YAG and Er: YAG laser approach: investigation of clinical and bone loss biomarkers, Dent. J. (Basel) 11 (3) (2023) 61, https://doi.org/10.3390/dj11030061. Feb 24PMID: 36975558; PMCID: PMC10046921.
[14] G. Xue, S. Wang, Q. Liu, K. Zhang, P. Xin, Analysis of the effects of concentrated growth factor and low-level laser therapy on the bone healing, Heliyon 9 (1) (2023) e12800, https://doi.org/10.1016/j.heliyon.2023.e12800. Jan 4PMID: 36691545; PMCID: PMC9860437.
[15] PF. Bradley, A review of the use of the neodymium YAG laser in oral and maxillofacial surgery, Br. J. Oral Maxillofac. Surg. 35 (1) (1997) 26–35, https://doi.org/10.1016/s0266-4356(97)90005-x. FebPMID: 9043000.
[16] A. De Filippis, A. D'Agostino, A.V.A. Pirozzi, M.A. Tufano, C. Schiraldi, A. Baroni, Q-switched Nd-YAG laser alone and in combination with innovative hyaluronic acid gels improve keratinocytes wound healing in vitro, Lasers Med. Sci. 36 (5) (2021) 1047–1057, https://doi.org/10.1007/s10103-020-03145-5.
[17] D.G. Pandurić, I. Bago, D. Katanec, J. Žabkar, I. Miletić, I. Anić, Comparison of Er: YAG laser and surgical drill for osteotomy in oral surgery: an experimental study, J. Oral Maxillofac. Surg. 70 (11) (2012) 2515–2521. Nov.
[18] H.B. Lopes, T.L. Rios, L.F. Adolpho, A.T.P. Souza, U.M. Lopes, E.H. Backes, et al., Evaluation of osteoblastic differentiation induced by microtextured titanium surface produced by laser metal fusion 3D printing, Mater. Res. 27 (2024), https://doi.org/10.1590/1980-5373-MR-2023-0448.
[19] P.H.S. Gomes-Ferreira, D. de Oliveira, P.B. Frigério, Souza de, F.R. Batista, K. Grandfield, R. Okamoto, Teriparatide improves microarchitectural characteristics of peri-implant bone in orchiectomized rats, Osteoporos. Int. 31 (9) (2020) 1807–1815, https://doi.org/10.1007/s00198-020-05431-y.

[20] S. Stopp, H. Deppe, T. Lueth, A new concept for navigated laser surgery, Lasers Med. Sci. 23 (3) (2008) 261–266, https://doi.org/10.1007/s10103-007-0476-4.
[21] J. Matys, J. Hadzik, M. Dominiak, Schneiderian membrane perforation rate and increase in bone temperature during maxillary sinus floor elevation by means of Er: YAG laser—an animal study in pigs, Implant Dent. 26 (2) (2017) 238–244, https://doi.org/10.1097/ID.0000000000000520.
[22] N. Muçulmano, A. Shahnaz, S. Masoumi, S. Torabi, S. Akbari, Laser-assisted osteotomy for implant site preparation: a literature review, Implant Dent. 26 (1) (2017) 129–136, https://doi.org/10.1097/ID.0000000000000475. Feb.
[23] J. Matys, R. Flieger, M. Dominiak, Assessment of temperature rise and time of alveolar ridge splitting by means of Er:YAG laser, piezosurgery, and surgical saw: an ex vivo study, Biomed. Res. Int. 2016 (2016) 9654975, https://doi.org/10.1155/2016/9654975.
[24] W.C.W. Chan, Z. Tan, M.K.T. To, D. Chan, Regulation and role of transcription factors in osteogenesis, Int. J. Mol. Sci. 22 (11) (2021) 5445, https://doi.org/10.3390/ijms22115445. May 21.
[25] T. Komori, What is the function of osteocalcin? J Oral Biosci 62 (3) (2020) 223–227, https://doi.org/10.1016/j.job.2020.05.004. Sep.
[26] T. Komori, Functions of osteocalcin in bone, pancreas, testis, and muscle, Int. J. Mol. Sci. 21 (20) (2020) 7513, https://doi.org/10.3390/ijms21207513. Oct 12.
[27] M.B. Chavez, M.H. Tan, T.N. Kolli, C. Zachariadou, F. Farah, F.F. Mohamed, et al., Bone sialoprotein is critical for alveolar bone healing in mice, J. Dent. Res. 102 (2) (2023) 187–196, https://doi.org/10.1177/00220345221126716. Feb.
[28] M. Schini, T. Vilaca, F. Gossiel, S. Salam, R. Eastell, Bone turnover markers: basic biology to clinical applications, Endocr. Rev. [Internet] 44 (3) (2023) 417–473, https://doi.org/10.1210/endrev/bnac031. May 8 [cited 2025 Jan 9]Available from, https://academic.oup.com/endo.
[29] D. Gabrić, D. Aumiler, M. Vuletić, E. Gjorgievska, M. Blašković, M. Mladenov, et al., Thermal evaluation by infrared thermography measurement of osteotomies performed with Er laser, piezosurgery and surgical drill—an animal study, Mater. (Basel) [Internet] 14 (11) (2021) 3051, https://doi.org/10.3390/ma14113051. Jun 3 [cited 2025 Jan 9]Available from, https://www.mdpi.com/journal/materials.
[30] M. Kawano, K. Wada, Y. Hemmi, S. Yokose, Effect of Nd:YAG laser on bone formation in rat tibia defects: three-dimensional micro-computed tomography image analysis, Lasers Med Sci [Internet] 38 (1) (2023) 158, https://doi.org/10.1007/s10103-023-03820-3. Jul 8 [cited 2025 Jan 9]Available from, https://link.springer.com/journal/10103.
[31] J. Matys, R. Flieger, G. Tenore, K. Grzech-Leśniak, U. Romeo, M. Dominiak, Er:YAG laser, piezosurgery, and surgical drill for bone decortication during orthodontic mini-implant insertion: primary stability analysis—an animal study, Lasers Med. Sci. [Internet] 33 (3) (2018) 489–495, https://doi.org/10.1007/s10103-017-2381-9. Apr [cited 2025 Jan 9]Available from, https://link.springer.com/journal/10103.